AN EFFICIENT ALGORITHM TO PREDICT THE EXPECTED END-OF- LIFE IN COMPOSITES UNDER FATIGUE CONDITIONS

M. Chiachio *[1], J. Chiachio[1], A. Saxena[2], G. Rus[1], K. Goebel[3]

[1] *Department of Structural Mechanics and Hydraulics Engineering , University of Granada, Granada, 18071, Spain*
[2] *SGT Inc. / Intelligent Systems Division, NASA Ames Research Center, Moffett Field, CA, 94035-1000, USA*
[3] *Intelligent Systems Division, NASA Ames Research Center, Moffett Field, CA, 94035-1000, USA*
* *Corresponding Author: mchiachio@ugr.es*

Keywords: Structural Health Management, Fatigue damage, model-based prognostics, Particle Filters,

Abstract
This work presents an efficient computational framework for estimating the end of life (EOL) and remaining useful life (RUL) by combining the prognostics principles with the technique of Subset simulation. It has been named PFP-SubSim on behalf of the full denomination of the computational framework, namely, particle filter-based prognostics using Subset Simulation. It is shown that the resulting algorithm is especially useful when dealing with the prognostics of evolving processes with asymptotic behaviors where the length of the dataset is limited, as observed in practice for many fatigue degradation processes in composites. Its efficiency is demonstrated on data collected from run-to-failure tension-tension fatigue experiments measuring the evolution of fatigue damage in CRFP cross-ply laminates using PZT sensors for obtaining data of matrix micro-crack density.

1. Introduction

Anticipating the serviceability in composite materials under fatigue loads is a challenge mainly due to the uncertainty in the multi-scale physics of the damage process and the large variability in behaviour that is observed. It requires the establishment of a prognostics framework to account for the observed variability into the predictions to be made about future states of damage.

The goal of prognostics is to make end of life (EOL) and remaining useful life (RUL) predictions of components, subsystems, and systems that enable timely maintenance decisions to be made under the presence of uncertainty [1]. In previous works by the authors [2, 3], a model-based prognostic framework is presented as a versatile way to deal with accurate long-term predictions for fatigue damage in composites. This framework implies complicated calibrations to tackle with the high dimensionality of the fracture-mechanic models that are simulated multiple times until a set of critical fatigue damage thresholds are reached. When the focus is on predicting a damage feature whose evolutive dynamic exhibits an asymptotic behaviour (like matrix micro-cracks density), the problem is exacerbated by the lack of prediction accuracy, unless a huge amount of samples are employed.

This work presents a novel efficient algorithm for estimating the EOL and RUL by combining the particle filter-based prognostics with the technique of Subset simulation, first developed in S.K. Au and J.L. Beck [4], resulting in a especially suited algorithm for the prognostics of matrix micro-cracks density and stiffness reduction for carbon-epoxy laminates under fatigue loads.

The idea behind this new algorithm, is to split the multi-step ahead predicted trajectories into multiple branches of selected samples at various stages of the future damage process, which correspond to increasingly closer approximations of the set of critical damage thresholds. As an application example, data collected from run-to-failure tension-tension fatigue experiments in CRFP cross-ply laminates, are used. Structural health monitoring in this example is accomplished through Lamb wave-based active interrogation using PZT sensors for obtaining data of matrix micro-crack density together with a set of strain-gauges for measuring stiffness reduction. The dataset used for this example is open-access dataset distributed by NASA Ames Prognostics Data Repository [5]. The results show that the new algorithm is efficient, and at the same time, fairly accurate in obtaining the PDFs of EOL and RUL since the beginning of the degradation process, precisely where previous approaches of prognostics in composites reported in the PHM literature fail in accuracy.

2. Damage growth models

A Fracture Mechanics approach based on a modified Paris law is adopted to model the rate of change of internal damage per cycle. Several authors [6] have adopted a modified Paris law to analyse the rate of damage growth in composites, which is intrinsically related with the energy released by the formation of a new crack between two existing cracks (termed as energy release rate). The energy release rate G, can be calculated based on different micro-damage mechanic models [6], like *shear-lag* models, *variational* models and *crack opening displacement* based models. In this work, the shear-lag approach is adopted for the calculation of G to be simpler and well-suited for symmetric cross-ply laminates[1]:

$$G = \frac{\sigma_x^2 h}{2\rho t_{90}} \left(\frac{1}{E_x^*(2\rho)} - \frac{1}{E_x^*(\rho)} \right) \tag{1}$$

where σ_x is the maximum applied axial tension, and h and t_{90} are the laminate and 90°-sublaminate half-thickness, respectively. The matrix micro-cracks density is defined by $\rho = \frac{1}{2\bar{l}}$, where $\bar{l}$ is the half crack-spacing normalised by the 90° sub-laminate thickness. The term $E_x^*(\rho)$, as a function of ρ, is the effective laminate Young's modulus due to the current damage state which can be calculated as:

$$E_x^* = \frac{E_{x,0}}{1 + a\frac{1}{2\bar{l}}R(\bar{l})} \tag{2}$$

In the last equation, the term a is defined as follows:

$$a = \frac{E_y h_{90}}{E_x h_\phi} \left(1 - \nu_{xy}^{(\phi)} \frac{\frac{\nu_{xy}^{(\phi)} h_{90}}{E_y^{(\phi)}} + \frac{\nu_{xy} h_\phi}{E_y}}{\frac{h_{90}}{E_y^{(\phi)}} + \frac{h_\phi}{E_x}} \right) \frac{1 - \nu_{xy}\nu_{xy}^{(\phi)}}{1 - \nu_{xy}^2 \frac{E_y}{E_x}} \tag{3}$$

[1]See last page for basic notation and relations

The function $R(\bar{l})$, known as the *average stress perturbation function*, is defined by [7]:

$$R(\bar{l}) = \frac{2}{\xi}\tanh(\xi\bar{l}), \text{ with } \xi^2 = G_{yz}\left(\frac{1}{E_y} + \frac{1}{\lambda E_x^{(\phi)}}\right) \tag{4}$$

For clearness, some terms involved in Equations 2 and 4 are grouped in Table 1. The remaining terms can be easily obtained by the laminate theory.

Next, the modified Paris' Law for the propagation of matrix cracks can be formulated as:

$$\frac{d\rho}{dt} = A(\triangle G)^{\alpha} \tag{5}$$

where A and α are fitting parameters. $\triangle(G)$ is the increment of energy release evaluated for the maximum and minimum stress in the cyclic load series: $\triangle(G) = G_{|\sigma_{max}} - G_{|\sigma_{min}}$. There is no closed-form solution for this differential equation, therefore we approximate the derivative by "unit-time" finite differences as:

$$\rho_t = \rho_{t-1} + A\,(\Delta G(\rho_{t-1}))^{\alpha} \tag{6}$$

3. Stochastic embedding

As discussed in the last section, the progression of damage is modeled at every cycle t by focusing on the matrix-cracks density, ρ_t, and the normalized effective stiffness, $D_t = \frac{E_x^*}{E_{x,0}}$, defining a joint response function of two components: $f_t = [f_{1_t}, f_{2_t}]$ for matrix cracks-density and normalized effective stiffness, respectively. Let denote by $x_t = [x_{1_t}, x_{2_t}]$ the actual system response, for matrix micro-cracks density and normalized effective stiffness, respectively. Next, the damage model is embedded stochastically [8] by adding a model-error term $v_t \in \mathbb{R}^2$ that represents the difference between the actual system response x_t and the model output f_t. The following state-space model is defined:

$$x_{1_t} = \rho_t = \underbrace{f_{1_t}(\rho_{t-1}, \theta)}_{\text{Equation 6}} + v_{1_t} \tag{7a}$$

$$x_{2_t} = D_t = \underbrace{f_{2_t}(\rho_t, \theta)}_{\text{Equation 2}} + v_{2_t} \tag{7b}$$

If $y_t = [y_{1_t}, y_{2_t}] = \left[\hat{\rho}_t, \hat{D}_t\right]$ are the measurements of the system output x_t, then the following measurement function is added to the discrete state-space model to account for the measurement error $w_t \in \mathbb{R}^2$:

$$y_{1_t} = \hat{\rho}_t = x_{1_t} + w_{1_t} \tag{8a}$$

$$y_{2_t} = \hat{D}_t = x_{2_t} + w_{2_t} \tag{8b}$$

We use the Principle of Maximum Information Entropy [8] to choose v_t and w_t as i.i.d. Gaussian variables, $v_t \sim \mathcal{N}(0, \left[\sigma_{v_{1_t}}, \sigma_{v_{2_t}}\right] I_2)$, $w_t \sim \mathcal{N}(0, \left[\sigma_{w_{1_t}}, \sigma_{w_{2_t}}\right] I_2)$, being $\left[\sigma_{v_{1_t}}, \sigma_{v_{2_t}}\right]$ and $\left[\sigma_{w_{1_t}}, \sigma_{w_{2_t}}\right]$ the variances of v_t and w_t respectively, and I_2 the identity matrix of order 2, so they can be readily sampled. For this example, we adopt $\sigma_{w_{1_t}} = 10^{-2}$ and $\sigma_{w_{1_t}} = 10^{-6}$, taking them as known.

In Equations 7 and 8, the model parameters θ are selected among the complete set of mechanical and geometrical parameters describing Equations 1 to 5 (see Table 1) through a Global Sensitivity Analysis based on variances and following the methodology proposed by [9]. The ply properties $\{E_x, E_y, h\}$ together with the fitting constant $\{\alpha\}$ emerged as sensitive parameters to model output uncertainty. To the last cited selection is added the variances of the model error function v_t, resulting in $\theta = \{\alpha, E_x, E_y, h, \sigma_{v_{1_t}}, \sigma_{v_{2_t}}\}$. The rest of parameters are fixed at any point within their range of variation, (e.g. the mean value) without significantly influencing the output uncertainty.

The recursion given by Equations 7 and 8 is typically evaluated by *particle filters* (PF) [10], whereby an approximation to the current PDF of states is readily obtained through a set of N discrete weighted particles, $\left\{\left(x_t^{(i)}, \theta_t^{(i)}\right), \omega_t^{(i)}\right\}_{i=1}^{N}$.

4. Damage prognostics

For predicting remaining useful life of a composite structure, we are interested in predicting the time when the damage grows beyond a predefined acceptable threshold. Using the most current knowledge of the system state at cycle $k \in \mathbb{N}$, which can be estimated by PF, the goal now is to estimate the PDF of EOL: $p(EOL_k|y_{0:k})$. The damage space itself may be defined by means of a set of thresholds $\mathbf{C} = \{C_1, \ldots, C_c\}$ on more than one critical parameters. In such cases, these thresholds can be combined into a *threshold function* $T_{EOL} : T_{EOL}(x, \theta, \mathbf{C})$ that maps a given point in the joint state-parameter space to the Boolean domain $\{0, 1\}$. For instance, when a given particle i starting from cycle k performs a random walk and hits any of the thresholds $\mathbf{C}$, then $T_{EOL}^{(i)} = 1$, otherwise $T_{EOL}^{(i)} = 0$. The time $t \geqslant k$ at which that happens defines the EOL for that particle. Mathematically:

$$EOL_k^{(i)} = \inf\{t \in \mathbb{N} : t \geqslant k \wedge T_{EOL}^{(i)}(x_k^{(i)}, \theta_k^{(i)}, \mathbf{C}_k) = 1\} \tag{9}$$

Using the updated weights at time, an approximation to the PDF of EOL is given by:

$$p(EOL_k|y_{0:k}) \approx \sum_{i=1}^{N} \omega_k^{(i)} \delta(EOL_k - EOL_k^{(i)}) \tag{10}$$

Examples of algorithmic description of the prognostic procedure based on PF can be found in the literature (eg. [11, 12]), to cite but a few. For convenience in notation, the augmented state $z = (x, \theta)$ in the joint state-parameter space is defined and used hereinafter.

5. Prognosis by Subset Simulation

Subset Simulation method is an efficient simulation framework originally proposed for computing small failure probabilities for general reliability problems [4]. It is motivated by the observation that the simulation of a rare event can be transformed into the simulation of successive intermediate events with larger probabilities. In Subset Simulation, the conditional probabilities are efficiently estimated by means of conditional samples that correspond to specified levels of the performance function g (defined in the last section) in a progressive manner.

Let us assume that there exist a specific failure region $\mathcal{F}$ into the state space that can be defined as the intersection of m nested regions in , i.e., $\mathcal{F}_1 \supset \mathcal{F}_2 \ldots \supset \mathcal{F}_{m-1} \supset \mathcal{F}_m = \mathcal{F}$, so that

$\mathcal{F} = \bigcap_{j=1}^{m} \mathcal{F}_j$. Each subset $\mathcal{F}_j$ (tipically termed as *intermediate failure domain*) is defined as $\mathcal{F}_j \equiv \{z_t \in : g(z_t) > C_j\}$, with $C_{j+1} > C_j$, such that $p(z_t|\mathcal{F}_j) \propto p(z_t)\mathbb{I}_{\mathcal{F}_j}(z_t)$, $j = 1, \ldots, m$. By definition of conditional probability, it follows that[2]:

$$P(\mathcal{F}) = P\Big(\bigcap_{j=1}^{m} \mathcal{F}_j\Big) = P(\mathcal{F}_1) \prod_{j=2}^{m} P(\mathcal{F}_j|\mathcal{F}_{j-1}) \tag{11}$$

where $P(\mathcal{F}_j|\mathcal{F}_{j-1}) \equiv P(z_t \in F_j | z_t \in F_{j-1})$, is the conditional failure probability at the $(j-1)^{th}$ intermediate failure domain, and denoted hereinafter by P_j for clearness.

To compute $P(\mathcal{F})$ based on 11, it is necessary to estimate the probabilities P_j, $j = 1, \ldots, m$. P_1 can be readily estimated by the standard Monte Carlo method (MC) as follows:

$$P(\mathcal{F}_1) \approx \bar{P}_1 = \frac{1}{M} \sum_{n=1}^{M} \mathbb{I}_{\mathcal{F}_1}(z_t^{0,(n)}) \tag{12}$$

where $z_t^{0,(n)}, n = 1, \ldots, M$, are samples from identically distributed multi-step ahead predicted trajectories simulated from $p(z_t)$. The superscript "0" here denotes that they are samples from the initial set simulated according to the model in Equation 7.

The remaining factors cannot be efficiently estimated using the MC method because of the conditional sampling involved. However, MCMC methods over the parameter θ can be used for sampling from the PDF $p(z_t^{j-1}|\mathcal{F}_{j-1})$ when $j \geqslant 2$, as:

$$P(\mathcal{F}_j|\mathcal{F}_{j-1}) \approx \bar{P}_j = \frac{1}{M} \sum_{n=1}^{M} \mathbb{I}_{\mathcal{F}_j}(z_t^{j-1,(n)}) \tag{13}$$

where $z_t^{j-1,(n)} \sim p(z_t^{j-1}|\mathcal{F}_{j-1})$ and $\mathbb{I}_{\mathcal{F}_j}(z_t^{j-1,(n)})$ is an indicator function for the region $\mathcal{F}_j$, $j = 1, \ldots, m$, that assigns a value of 1 when $g(z_t^{j-1,(n)}) > C_j$, and 0 otherwise.

Observe that it is possible to obtain Markov chain samples that are generated at the $(j-1)^{th}$ level which lie in the subsequent level $\mathcal{F}_j$. They are samples conditional on $\mathcal{F}_j$ and provide "seeds" for simulating more samples according to $p(z_t|\mathcal{F}_j)$ by using MCMC sampling with no burn-in required, which is an important feature of Subset Simulation to avoid wasting samples [13, 4]. We adopt the method of establishing the intermediate levels $\mathcal{F}_j$ adaptively so that $P(\mathcal{F}_j|\mathcal{F}_{j-1}) \approx P_0 \in [0, 1]$ (see more details in [13]).

5.1. The PFP-SubSim algorithm

Let suppose that a sequence of measurements up to time k, $y_{0:k}$, are given and that a PF filter approximation based on N particles is obtained for the current PDF of states. Fix the conditional probability parameter P_0 (eg. $P_0 = 0.2$ [13]) that entails the set of nested failure regions $\mathcal{F}_j \subseteq \mathcal{F}$, $j = (1, \ldots, m)$. Proceed as follows:

1.- Generate M predicted samples at time $t > k$, $\left\{z_t^{0,(1)}, \ldots, z_t^{0,(n)}, \ldots, z_0^{0,(M)}\right\}$ using the recursion in Equation 7 (it is considered as the initial subset $j = 0$).

[2]In what follows, we use $P(\cdot)$ to denote probability whereas a PDF is expressed as $p(\cdot)$. In addition, we use $P(F) \equiv P(z \in F)$, for simpler notation

while $j = 0$ or $C_j < C$ **do**
  $j \leftarrow j + 1$
  2.- Evaluate the performance function g over the last set: $g_j^{(n)} = g\left(z_t^{j-1,(n)}\right)$.
  3.- Sort $g_j^{(n)}$ so that $g_j^{(1)} \leqslant g_j^{(2)} \leqslant \dots g_j^{(N)}$ and fix $C_j = \frac{1}{2}\left(g_j^{(MP_0)} + g_j^{(MP_0+1)}\right)$.
  4.- Select the subset of samples $\mathcal{Z}_j : \{z_t^{j,(1)}, \dots, z_t^{j,(M_1)}\}, M_1 \leqslant M$, verifying $g_j^{(n)} \leqslant C_j$, $n = 1, \dots, M_1$.
  5.- Starting from the samples in $\{\mathcal{Z}_j\}$ considered as seeds, reproduce them using Eq. 7 to obtain a new set of M samples for the $(j + 1)^{th}$ level (or just the final level when $j = m$).
  if $b_{j \geqslant} C$ **then**
    6.- Record the times indexes $t > k \in \mathbb{N}$ of the first-passage points→End Algorithm
  end if
end while

The collection of time indexes of the final subset ($j = m$) forms a discrete set for the approximation of the PDF of EOL as states in Equation 10.

6. Results and conclusions

The proposed framework was applied to fatigue cycling data for cross-ply graphite-epoxy laminates. Torayca T700G uni-directional carbon-prepreg material was used for 15.24 [cm] x 25.4 [cm] coupons with dogbone geometry. The tests were conducted under load-controlled tension-tension fatigue loadings with a frequency of $f = 5$ [Hz], a maximum stress of 80% of their ultimate stress, and a stress ratio $R = 0.14$. The whole parameter set-up is summarised in Table 1.

Type	Parameter	Nominal value	Units	COV (%)	Prior PDF
Mechanical	E_x	127.55	GPa	10	LN
	E_y	8.41	GPa	10	LN
	G_{xy}	6.20	GPa	10	LN
	$\frac{G_m}{d_0}$	$1 \cdot 10^5$	GPa/m	50	LN
	ν_{xy}	0.31	–	10	LN
	G_{yz}	2.82	GPa	10	LN
	h	$1.5 \cdot 10^{-4}$	m	10	LN
Fitting	α	1.80	–	20	LN
	A	$1 \cdot 10^{-4}$	–	20	LN
Errors	$\sigma_{v_{1_t}}$	4	$\frac{\text{\# cracks}}{m \cdot \text{cycle}}$	–	$U(0.5, 8)$
	$\sigma_{v_{2_t}}$	0.01	$\frac{\text{\# cracks}}{m \cdot \text{cycle}}$	–	$U(0.001, 0.02)$

Table 1. Prior information and nominal values of main parameters used in calculations. Classical laminate theory may be use from these parameter to obtain the remaining parameters attributable to the laminate configuration.

Lamb waves signals were periodically recorded using a PZT sensor network to estimate internal microcrack density. The mapping between PZT raw data and microcrack density was done following the methodology proposed in [14]. In addition, macro-scale damage measurements were taken using strain gauges at periodic intervals interspersed between fatigue cycling experiment. In this study, a threshold value of matrix micro-cracks density of $\rho = 424.5$ cracks per meter is considered. The results are presented for three different simulation levels ($m = 3$) in Figure 1(a), by using $P_0 = 0.2$ and $M = 2.4 \cdot 10^4$ samples per simulation level.

Fatigue cycles, n	10^1	10^2	10^3	10^4	$2{\cdot}10^4$	$3{\cdot}10^4$	$4{\cdot}10^4$	$5{\cdot}10^4$	$6{\cdot}10^4$	$7{\cdot}10^4$	$8{\cdot}10^4$	$9{\cdot}10^4$	10^5
ρ_n [$^{\#\text{ cracks}}/_{m}$]	98.2	111.0	117.4	208.5	269.6	305.0	355.5	396.4	402.3	402.1	407.0	418.5	424.5

Table 2. Experimental sequence of damage for cross-ply $[0_2/90_4]_s$ Torayca T700 CFRP laminate taken from the Composite dataset, NASA Ames Prognostics Data Repository [5]. The data are presented for micro-cracks density (ρ_n corresponding to specimen L1S19 in the dataset.)

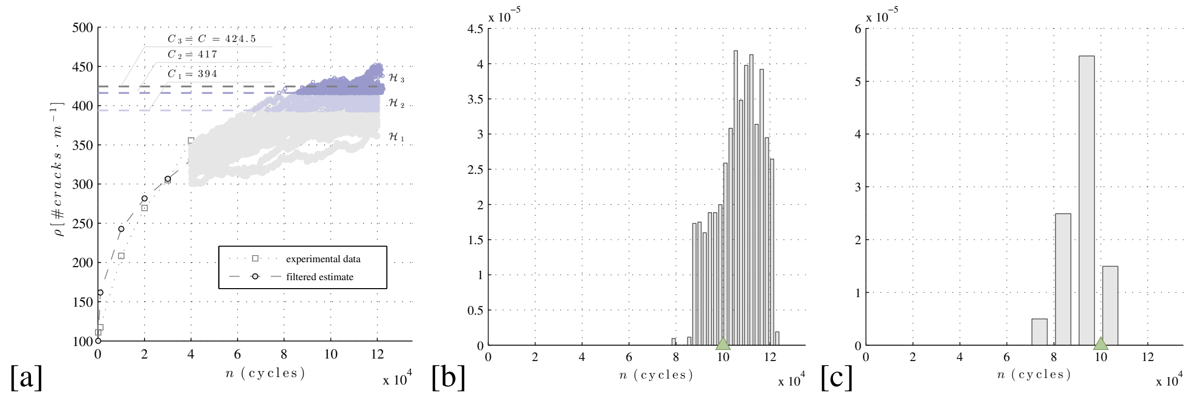

Figure 1. Prognostics results for predicting matrix micro-cracks density from cycle $k = 4 \cdot 10^4$ using the modified Paris' law model. (a): PFP-SubSim output using $M = 2.4 \cdot 10^4$ samples per simulation level. Each subset is defined by samples (circles) in the micro-cracks (ρ) space, where the latest intermediate predictive samples are marked in dark purple circles. (b): Histogram representation of the estimated EOL at cycle $k = 4 \cdot 10^4$ using PFP-SubSim algorithm. The green triangle represents the time (in cycles) when matrix micro-cracks density will reach the final threshold $C = 424.5$ [$\#cracks \cdot m^{-1}$], which is known off-line from [5] (laminate L1S19), and also shown in Table 2. (c) Histogram representation of the estimated EOL at cycle $k = 4 \cdot 10^4$ calculated using $7.2 \cdot 10^4$ samples without using PFP-SubSim algorithm being used.

The results shown in Figure 1(a) and (b) are satisfactory in the sense that our algorithm has the ability to estimate the EOL with high statistical precision with a moderate computational cost. In Figure 1(c), a prognostic evaluation is done using the same total number of model evaluations as when PFP-Algorithm is adopted, i.e. $M = 3.4 \cdot 10^4 = 7.2 \cdot 10^4$ samples. Observe that the histogram representation of the EOL estimate is quite poor when FPF-SubSim algorithm is not used, and only a better estimate may be obtained by employing more simulations, which necessarily increases the computational cost. This computational issue is a common aspect of prognostics of asymptotic processes, overall when conservative (or unprovable) threshold levels are adopted. These results suggest that high efficiency can be gained by employing the PFP-SubSim algorithm for prognostics of matrix micro-density in composite materials.

Acknowledgements

The authors would like to thank the European Union for the Programa Operativo FEDER de Andalucía 2007-2013 for project GGI3000IDIB and to the Prognostics Center of Excellence at NASA Ames, which kindly hosted them during the course of this work. Authors would also like to thank Structures and Composites lab at Stanford University for experimental data and NASA ARMD/AvSafe project SSAT, which provided partial support for this work.

References

[1] John D Kalbfleisch and Ross L Prentice. *The statistical analysis of failure time data*. John Wiley & Sons, 1980.

[2] J. Chiachío, M. Chiachío, A. Saxena, G. Rus, and K. Goebel. An energy-based prognostics framework to predict fatigue damage evolution in composites. In *Proceedings of the Annual Conference of the Prognostics and Health Management Society, 2013*, volume 1, pages 363–371. Prognostics and Health Management Society, 2013.

[3] M. Chiachío, J. Chiachío, A. Saxena, G. Rus, and K. Goebel. Fatigue damage prognosis in FRP composites by combining multi-scale degradation fault modes in an uncertainty Bayesian framework. In *Proceedings of Structural Health Monitoring, 2013*, volume 1, 2013.

[4] S.K. Au and J.L. Beck. Estimation of small failure probabilities in high dimensions by *S*ubset *S*imulation. *Probabilistic Engineering Mechanics*, 16(4):263–277, 2001.

[5] A Saxena, K Goebel, C Larrosa, and FK Chang. CFRP Composites dataset, 2008. NASA Ames Prognostics Data Repository, [http://ti.arc.nasa.gov/project/prognostic-data-repository], NASA Ames, Moffett Field, CA.

[6] Ramesh Talreja and Chandra Veer Singh. *Damage and failure of composite materials*. Cambridge University Press, 2012.

[7] R Joffe and J Varna. Analytical modeling of stiffness reduction in symmetric and balanced laminates due to cracks in 90 layers. *Composites Science and Technology*, 59(11):1641–1652, 1999.

[8] J.L. Beck. *B*ayesian system identification based on probability logic. *Structural Control and Health Monitoring*, 17(7):825–847, 2010.

[9] Andrea Saltelli, Marco Ratto, Terry Andres, Francesca Campolongo, Jessica Cariboni, Debora Gatelli, Michaela Saisana, and Stefano Tarantola. *Global Sensitivity Analysis: The Primer*. Wiley-Interscience, 2008.

[10] NJ. Gordon, DJ Salmond, and AFM Smith. Novel approach to nonlinear/non-Gaussian Bayesian state estimation. *IEEE-Proceedings-F*, 140:107–113, 1993.

[11] Mathew Daigle and Kai Goebel. Model-based prognostics with fixed-lag particle filters. In *Proceedings of the Annual Conference of the Prognostics and Health Management Society, 2019*, volume 1, pages 249–261, 2009.

[12] Marcos Orchard, Gregory Kacprzynski, Kai Goebel, Bhaskar Saha, and George Vachtsevanos. Advances in uncertainty representation and management for particle filtering applied to prognostics. In *International conference on prognostics and health management*. IEEE, 2008.

[13] K.M. Zuev, J.L. Beck, S.K. Au, and L.S. Katafygiotis. *B*ayesian post-processor and other enhancements of *S*ubset *S*imulation for estimating failure probabilities in high dimensions. *Computers & Structures*, 93:283–296, 2011.

[14] C Larrosa and FK Chang. Real time in-situ damage classification, quantification and diagnosis for composite structures. In *Proceedings of the 19th* I*nternational* C*ongress on* S*ound and* V*ibration*, volume 15, 2012.